Proceedings of the ASME 2010 3rd Joint US-European Fluids Engineering Summer Meeting and 8th International Conference on Nanochannels, Microchannels, and Minichannels
FEDSM-ICNMM2010
August 1-5, 2010, Montreal, Canada

FEDSM-ICNMM2010-30193

FLOW VISUALIZATION AND PIV MEASUREMENTS OF FLOW AROUND A SPORT UTILITY VEHICLE MODEL

Alban Lamy
Mechanical Engineering
University of Ottawa
Ottawa, ON, Canada

Amandine Hamel
Mechanical Engineering
University of Ottawa
Ottawa, ON, Canada

Christina Vanderwel
Mechanical Engineering
University of Ottawa
Ottawa, ON, Canada

Stavros Tavoularis
Mechanical Engineering
University of Ottawa
Ottawa, ON, Canada

Azeddine Kourta
Institut PRISME
Polytech'Orléans
Orléans, France

ABSTRACT

The instantaneous flow structure around a 1:18 scaled model of a square-back sport utility vehicle (Hummer H2) was documented in a low-speed water tunnel. The study comprises both flows with the model fixed on a flat plate and flows with the model's wheels rolling on an endless belt that moved with the speed of the free stream, thus simulating ground effects. The flow structure was investigated using flow visualization by dye injection as well as particle image velocimetry (PIV) for several Reynolds numbers in the range of 7000 to 27700. The flow along the roof, the sidewalls, and the underbody was observed to separate at the rear edges of the body, creating a recirculation zone at the rear of the vehicle, which is associated with pressure loss and a major contribution to aerodynamic drag. In the vertical plane of symmetry, this recirculation zone appears as two counter-rotating vortices. With a fixed ground, the lower vortex was less energetic than the upper vortex because the boundary layer that developed along the ground upstream of the model reduced the momentum of the flow below the vehicle. This boundary layer was also observed to separate from the ground behind the vehicle, creating a third vortex located further downstream along the ground. This boundary layer separation forced the bottom vortex to remain attached to the base of the vehicle, whereas the upper vortex was advected in the wake. The dimensionless frequency (Strouhal number) of the vortex shedding process from the roof was found to be in the range of 0.1 to 0.9. With a moving ground, the upper vortex behaved similarly to that in the fixed ground configuration; however, in the absence of the boundary layer along the ground, the lower vortex was typically stronger and its location showed some variability. In both configurations, the Reynolds number had little influence on the wake topology, mostly increasing the turbulence intensity without modifying the main flow pattern.

NOMENCLATURE

f	Frequency of vortex shedding
G	Gap height between the vehicle and the ground
H	Height of the vehicle from the underbody to the roof
L	Streamwise length of the vehicle
Re_L	Reynolds number based on model length
St	Strouhal number
U_o	Upstream flow velocity
W	Width of the vehicle
x	Streamwise position

INTRODUCTION

The aerodynamic characteristics of ground vehicles are an important consideration in the design of road vehicles. In particular, it is desirable to keep the aerodynamic drag as low as possible, as this would also minimize fuel consumption and greenhouse gas emissions. Reducing unsteady aerodynamic loading would also be beneficial to the vehicle's handling capabilities and riding comfort.

Aerodynamic drag is composed of skin friction drag, form drag and induced drag. The relative magnitudes of these three drag components depend strongly on the shape of the vehicle. For road vehicles with a bluff shape, form drag is usually dominant. This drag arises from the low pressure in the wake of the vehicle, which forms by flow separation from the rear of

the vehicle's body. Even though passenger vehicles have relatively low total lift (or downthrust), streamwise vortices in their wakes generate an induced drag, which accounts for 8 to 28% of the total drag (Ahmed, 1981).

One of the most important factors that affect aerodynamic drag is the shape of the vehicle's rear, as this has a direct effect on flow separation and the formation of vortices in the wake. The proximity of the vehicle to the ground, wheel rotation, and the presence of accessories protruding from the vehicle's exterior also affect the near-wake flow and the aerodynamic drag.

The objective of this study is to document experimentally the instantaneous structure of the wake of a realistic square-back vehicle model, taking into account the effect of exterior detailing as well as ground effects and wheel rotation on the vortex development. Analysis of the instantaneous flow structure, rather than the time-averaged flow, is required to provide insight into the aerodynamic stability of the vehicle and vortex structure interactions, and to guide strategies for flow control (Krajnovic and Davidson, 2005). Although some of the flow patterns may be specific to the shape of this model, it is expected that, qualitatively, the wake topology would be similar for other vehicles with square-back rear geometries. A long-term objective is to develop and test experimentally passive and active methods of controlling flow separation from square-back vehicles (Gilliéron and Kourta, 2010).

BACKGROUND

The general characteristics of the wake of a ground vehicle are similar to those of simplified two-dimensional bluff bodies, which have been studied widely (e.g., Bosch et al., 1996; Bailey et al., 2002). In two-dimensional flow around a square cylinder at sufficiently large Reynolds numbers, the flow separates at the front edges of the cylinder and creates a large recirculation zone in the rear. Vortices are shed periodically from either side of the cylinder and get convected in the wake in the form of a von Kármán vortex street. The dimensionless frequency of vortex shedding is expressed as the Strouhal number

$$\mathrm{St} = \frac{f H}{U_0}, \qquad (1)$$

where f is the frequency of vortex shedding, H is the height of the body, and U_0 is the free stream velocity. In addition to the primary vortex shedding process, other modes of instability may arise in the vortex motions.

The introduction of an impenetrable boundary adjacent to the body alters the wake characteristics. As the gap width G between the body and the wall decreases in relation to the height H of the body, the boundary layer that develops along the wall reduces the fluid momentum in the gap region and weakens the shear on its side of the wake. When the relative gap width G/H drops below a critical value, vortex shedding from the near-wall side of the body is suppressed. For a square cylinder at a Reynolds number of 22000, the critical gap width is in the range of $0.35 < G/H < 0.50$ (Bosch et al., 1996).

The wake of a passenger car is much more complex than that of a two-dimensional body. The three-dimensional flow around a bluff body of finite aspect ratio alters the wake topology and drag of the bluff body, as well as the characteristics of periodic phenomena (Martinuzzi and Tropea, 1993; Shah and Ferziger, 1997). Previous studies of three-dimensional vehicle geometries (e.g., Ahmed, 1981; Carr, 1983; Hucho and Sovran, 1993; Bearman, 1997; Howell, 2005; Guilmineau, 2008; Guilmineau and Chometon, 2009; Rouméas et al., 2009) observed flow separation at the rear of the body, resulting in a large recirculation zone. In a central vertical plane, this zone is divided into counter-rotating upper and lower regions of recirculation, whose relative strengths depend on the rear geometry of the vehicle. In a central horizontal plane, regions of recirculation also form as the flow separates from the sides of the vehicle. Viewed as a whole, the three-dimensional wake contains a large vortex ring, which, in cross-section, appears to consist of a counter-rotating vortex pair.

For certain body shapes, velocity measurements beyond the recirculation zone have identified the presence of quasi-streamwise trailing vortices, originating on the lateral edges of a sloped windshield or a slanted rear surface. The characteristics of these trailing vortices and the magnitude of the induced drag they generate depend strongly on the vehicle geometry. Instantaneous measurements of velocity fields in a cross-flow plane have identified multiple, wandering, compact trailing vortices (Bearman, 1997). Despite their unsteadiness, these vortices have an effect on the time-averaged drag. For some notch-back vehicles, the trailing vortices generate a mean downwash between them that postpones flow separation and reduces the pressure drag. However, this is not the case for square-back vehicles, which actually produce a small upwash in the time-mean (Ahmed, 1981). One strategy of aerodynamic design, described by Hucho and Sovran (1993) and recently investigated by Aider et al. (2010), is to minimize the effect of these trailing vortices in order to minimize the induced drag.

Surface details (e.g., radiator grilles, underbody parts, mirrors, and door handles), which form protrusions or cavities on the exterior of road vehicles, further complicate the vehicle's aerodynamic characteristics (Carr, 1983). Such flow obstructions may produce local shear layers, separation regions and steady or unsteady vortices, which may interact with each other and affect in a complex manner the near-wake flow and the aerodynamic drag. Ahmed (1981) found that the addition of surface details to a vehicle model increased the total drag by 66% to 98%. Howell (2005) reports that for sport utility vehicles (SUVs), the addition of off-road accessories such as roof racks, a schnorkel, bug deflector, mudflaps, and nudge bars further increases the drag by 50% of that of the base model.

Finally, the effect of the moving ground is important to the wake topology (Hucho and Sovran, 1993). Most previous experimental studies of the flow around ground vehicles have

considered a stationary ground. Bearman et al. (1989) found that a simplified bluff-body model mounted on a moving ground experienced an 8% decrease in drag and a 30% decrease in lift with respect to measurements with a stationary ground. The magnitudes of these effects were found to depend on the rear and underbody vehicle geometries as well as the gap height between the vehicle and the ground. The rotation of the wheels contributes to this effect by changing the drag by up to 2% with respect to models with stationary wheels, depending on the vehicle geometry and the wheelhousing size (Cogotti, 1983).

EXPERIMENTAL FACILITIES AND PROCEDURES

All experimental work was conducted at the University of Ottawa's closed-loop, variable-speed water channel. The test section has a free surface and three glass walls forming a channel that is 0.53 m wide and 4.0 m long that was kept with a water depth of 0.61 m throughout all experiments.

A Hummer H2 was chosen as representative of square-backed sport utility vehicles, due to the availability of a well-built, detailed scaled model. A 1:18 scale model was used, which fit easily within the channel, having a frontal area of about 2.5% of the channel cross-section. Its dimensions are reported in Fig. 1, and correspond to a non-dimensional gap ratio of G/H = 0.375.

In order to investigate the flow with a stationary ground, the model was submerged into the water and fastened upside-down to a smooth steel plate positioned slightly below the free surface. The steel plate had a beveled leading edge to prevent flow separation and was 0.76 m long and 0.34 m wide. The model was positioned centrally on the plate.

To study flows with a moving ground, the model was mounted such that its wheels were in contact with, and rolling on, a horizontal endless belt, inserted in the water just below the free surface. The belt speed was adjusted to match the free-stream velocity. The experiments were conducted at several Reynolds numbers (based on the free-stream velocity upstream of the model and the model length) in the range $7000 < Re_L < 27700$, which corresponds to upstream velocities in the range $0.02 \text{ m/s} < U_0 < 0.11 \text{ m/s}$.

Visualization of the model's wake and other flow patterns was achieved by injecting neutrally buoyant dye into the flow, which formed visible streaklines. Two dyes were used: Congo red dye, which provided good visibility of the 3D flow structure when illuminated by flood light against a white background; and Fluorescein disodium salt, which is a fluorescent dye providing excellent visibility when illuminated by an Ar-ion laser sheet at a wavelength of 495 nm. In both cases, the dye was introduced isokinetically using a thin tube positioned upstream of the model, or from orifices within the model.

Particle image velocimetry (PIV) measurements were conducted using a 2D planar system (FlowMaster, Imager Pro X 4M, LaVision Inc., Göttingen, Germany), which has a maximum sampling rate of 7.24 Hz. The field of view was adjusted to approximately 200 mm × 200 mm in order to capture the entire wake of the car, resulting in a spatial resolution of about 3.5 mm. Silicon carbide particles, with a diameter of about 2 μm, were used to seed the flow. From the velocity field, the vorticity and swirling strength fields were calculated to help identify coherent vortices in the wake.

RESULTS

The main coherent structures observed in the wake of the square-back car model are in agreement with the literature. The flow along the roof, sidewalls and underbody separated on the rear edges of the body, forming a large, vortex-ring-like recirculation zone, which expanded over the entire base of the model. On either the vertical or the horizontal median planes, the recirculation zone appeared to consist of two counter-rotating regions (Fig. 2). Further downstream, a saddle point

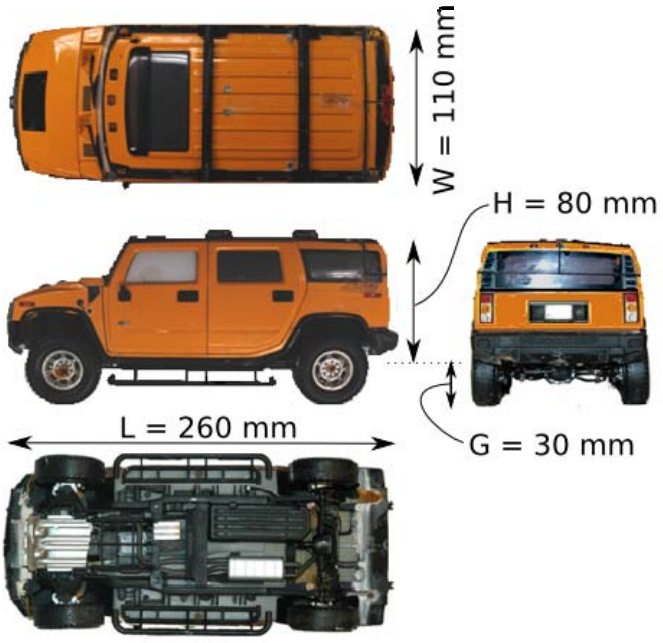

Figure 1: Photographs of the model, also showing the main dimensions.

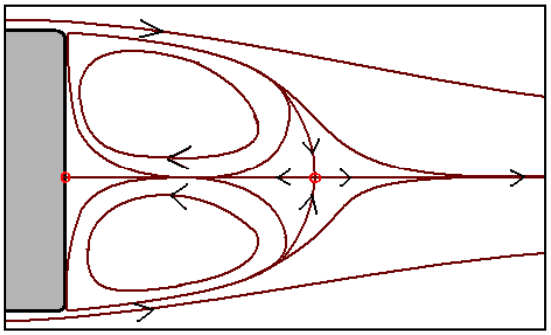

Figure 2: Sketch of the general wake topology in either the vertical or horizontal median planes.

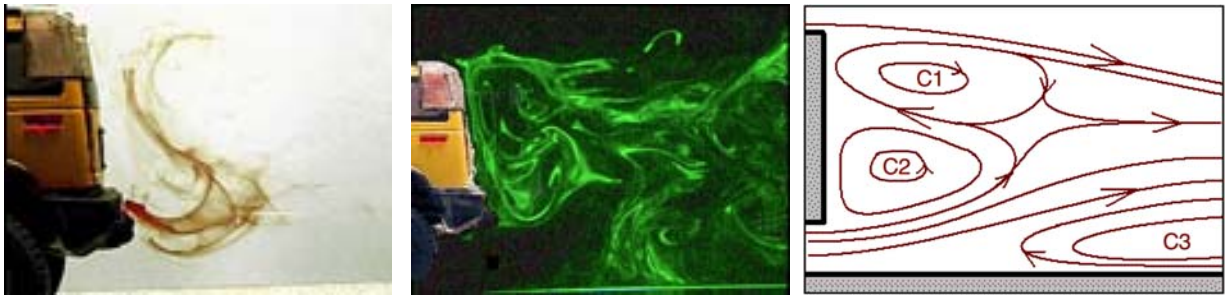

Figure 3: Flow visualization images using Congo red dye (left) and fluorescent dye (center), and a simplified sketch of the wake topology (right) in a vertical plane with a stationary ground.

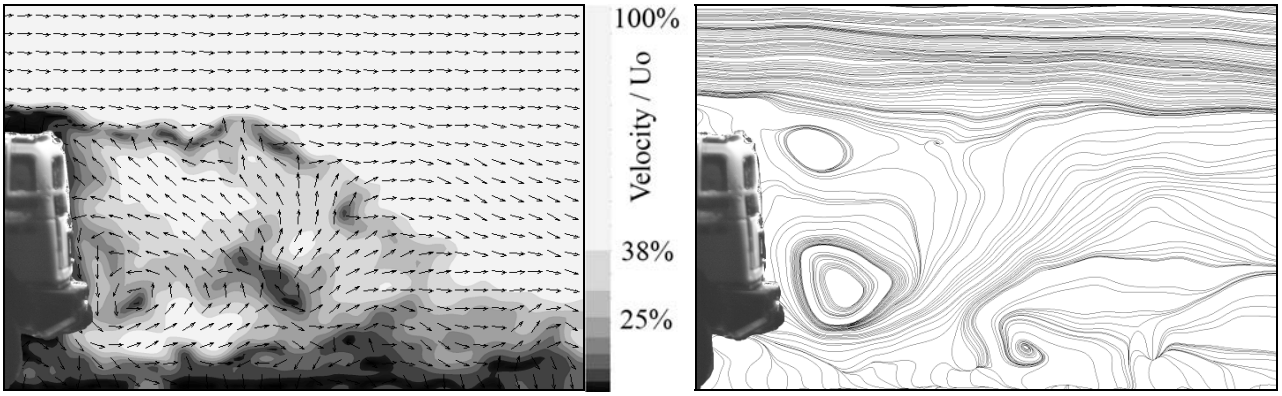

Figure 4: PIV measurements in the vertical median plane with a stationary ground, showing a velocity map (left) and streamlines (right).

appeared. A recirculation length could be defined as the distance between the saddle point and the reattachment point on the base. The recirculation length and the characteristics of the recirculation zone depended on the relative motions of the ground and the wheels.

Stationary Ground

In the vertical plane, the flows along the roof and the underbody separate at the rear edges of the body, which generate an upper vortex (C1) and a lower vortex (C2) (Fig. 3). The vertical position of the reattachment point depends on the relative characteristics of these two vortices.

With a fixed ground, a boundary layer develops along the ground surface. This reduces the flow momentum in the gap region, and makes the lower vortex weaker than the upper vortex, in agreement with earlier work (Rouméas et al., 2009).

The interaction of the boundary layer with the adverse pressure gradient in the wake of the vehicle causes flow along the ground to separate at a distance of about 1H downstream of the base. This separation forms a third vortex (C3) along the ground in the far wake of the vehicle. This topology is easily identified in the dye visualizations presented in Fig. 3. These characteristics are also observed in the flow maps measured with PIV, one of which is presented in Fig. 4. The lower vortex remained at essentially the same position in all measurements. This stability of the lower vortex is attributed to the separation of the ground boundary layer.

The upper vortex, however, was less stable. In some PIV recordings, several vortices were observed in the upper part of the recirculation zone, which indicates that the upper vortex became detached and was convected downstream. The Strouhal number of this vortex shedding process was in the range from 0.1 to 0.9, depending on the flow Reynolds number. This measurement was subject to a relatively large uncertainty, partially due to difficulty in tracking the downstream motion of the vortices and partially due to the intermittency of the shedding. The ground clearance of the Hummer model is G/H = 0.375, which, according to Bosch et al. (1996), is in the transition region between steady flow and fully periodic shedding for two-dimensional flow around a square-shaped body.

Planar PIV measurements taken in vertical planes offset from the mid-plane (not presented here) showed that the structures remained coherent for 55% of the vehicle width, centered at the mid-plane. This is consistent with the observed formation of a vortex ring in the recirculation zone, which had sections nearly parallel to the roof and the bottom of the model.

In a horizontal plane, the flows along the sides of the vehicle were also observed to separate at the rear of the vehicle (Fig. 5). Two counter-rotating vortices were visible on this

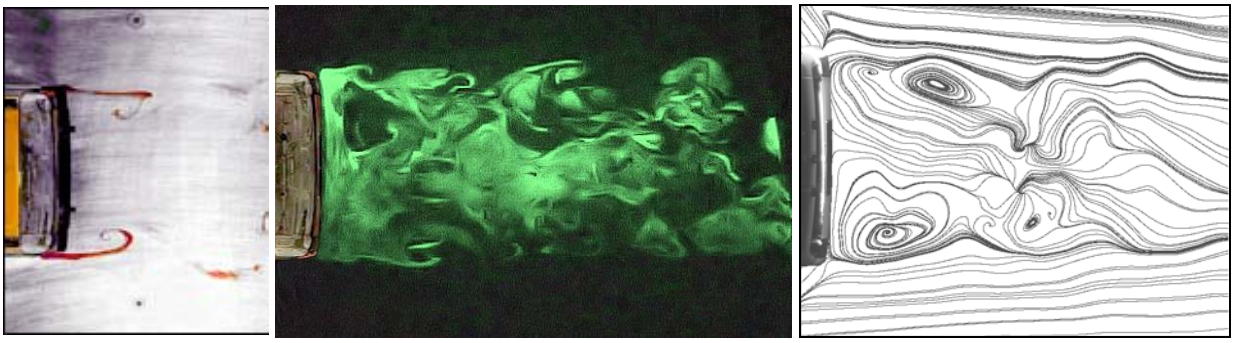

Figure 5: Flow visualization images (left and center) and PIV-generated streamlines (right) in the mean horizontal plane with a stationary ground.

plane, with the fluid between them moving in the upstream direction, resembling the observations of Gohlke et al. (2007) with a simplified square-backed model with no crosswind. This primary structure remained stable throughout the observations, although the vortices were sometimes observed to split into multiple smaller vortices, some of which were convected in the wake. Once shed, these vortices were often indistinguishable from vortices generated through Kelvin-Helmholtz instability along the shear layers bounding the wake. Their convection velocities depended on their positions in the wake such that the further they were from the center of the recirculation zone, the faster they moved downstream. As these vortices are in motion, they are not visible in the PIV-generated streamlines of Fig. 5, but can be viewed in the streaklines of the dye visualization. These vortices were shed simultaneously from both sides of the vehicle, with a frequency corresponding to a Strouhal number between 0.5 and 1.

The results obtained from the vertical and horizontal planes suggest the formation of a vortex ring behind the car, which is in agreement with the computational results of Rouméas et al. (2009). The bottom part of this vortex ring seems to remain attached, whereas the upper part and the sides of the vortex ring detach periodically, as observed by their convection in the wake.

Visualizations in a transverse plane through the wake of the vehicle show secondary instabilities (Fig. 6). At a distance of $x/H = 0.1$ from the rear of the vehicle, vortices were observed at the bottom corners, which seemed to dissipate very quickly and were not noticeable any further downstream. At a downstream position of $x/H = 1$, secondary instabilities were observed, similar to the B-mode instabilities observed in the wake of a square cylinder. They appeared as pairs of counter-rotating vortices linked to each other and disappeared very quickly. This unsteady and short-lived motion suggests that the quasi-streamwise trailing vortices do not have a large effect, which agrees with Ahmed (1981) who reports that for square-backed vehicles the induced drag comprises only 8% of the total drag.

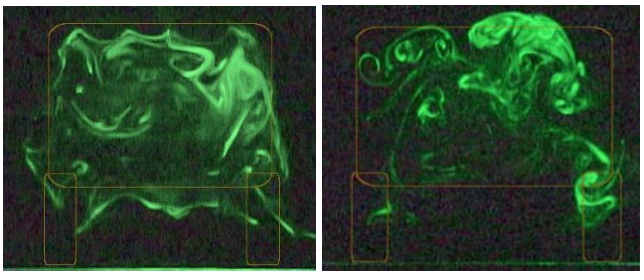

Figure 6: Fluorescent dye visualization in the transverse plane at a distance of x/H = 0.1 (left) and x/H = 1 (right) from the base, with Re_L = 7000 and a stationary ground.

Moving Ground

Because the moving ground had the same velocity as the upstream flow, no boundary layer formed on the ground upstream of the model. The high-velocity stream leaving the underbody under the recirculation zone remained attached to the ground, although some fluid behind the rotating wheels lifted upwards due to the wheel rotation. As the flow did not separate from the ground, the near wake appeared more symmetric than that with the stationary ground. The recirculation length was about 2H, significantly longer than that for the fixed-ground case, which was about 1.35H.

In the vertical median plane, the flow separated from the top and the bottom of the model and formed a large recirculation zone consisting of two counter-rotating regions, just as with the stationary ground. With the moving ground, however, the lower vortex (C2) was energized by the near-ground flow and appeared to have nearly the same strength as the upper vortex (C1). Nevertheless, the near-wake of the model appeared to be less stable, as both upper and lower vortices were convected in the wake. These vortices are visible in dye visualization images (Fig. 7) along both the upper and lower edges of the wake.

The instability of the wake topology is also apparent in the instantaneous velocity maps and streamline patterns obtained with PIV (Fig. 8). Multiple clockwise vortices are observed in the upper wake, and multiple counter-clockwise vortices can be seen in the lower wake. The convection speed of these vortices

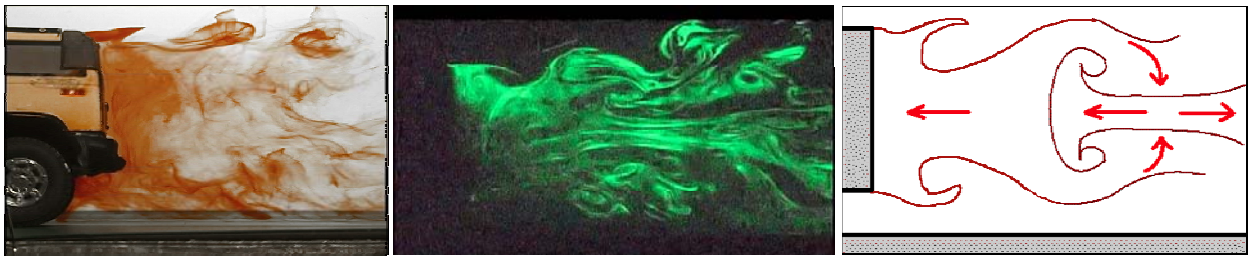

Figure 7: Dye visualization and a simplified sketch of the wake topology in the mean vertical plane with a moving ground.

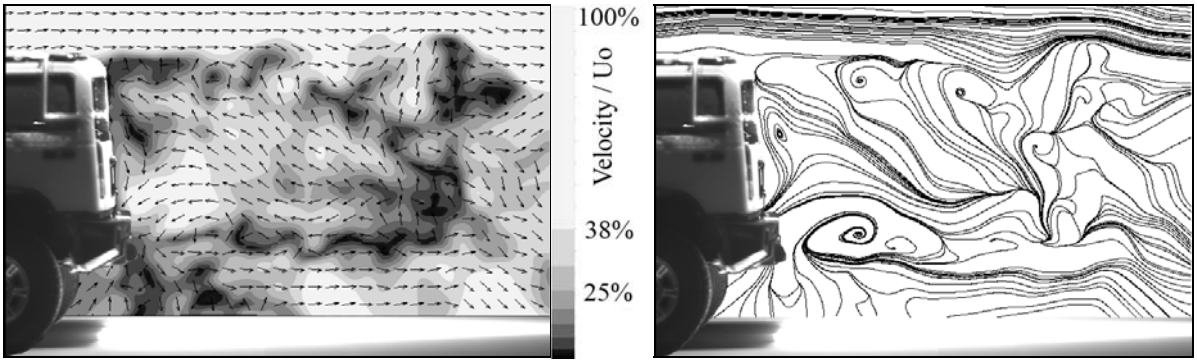

Figure 8: PIV measurement of the instantaneous wake topology in the mean vertical plane with a moving ground, showing velocity (left) and streamlines (right).

fluctuated and the vortices also wandered vertically, sometimes reaching vertical distances from the ground that were larger than those for the fixed-ground case. At the particular instant presented in Fig. 8, a counter-clockwise vortex (C2) was located at the centre of the rear face of the vehicle, creating a downward flow along the rear window of the vehicle. At the same instant, the reversed flow was inclined towards the roof of the model, resulting in an asymmetry of the wake. At other time instances, the wake was nearly symmetric and the reversed flow impinged upon the centre of the rear face of the model. Such an instance was captured with the fluorescent dye visualization shown in Fig. 7 and is illustrated by the accompanying sketch.

In a horizontal median plane, this recirculation zone was composed of two counter-rotating vortices separated by a counter flow in a manner that did not differ significantly, at least in topology, from the results obtained with a fixed ground.

Just as with the stationary ground, the results suggest the formation of a vortex ring behind the car. In the moving ground case, however, the lower part of the recirculation zone was not very different from the upper part. The same vortex shedding frequency (St ≈ 1) has been observed in both the upper and lower shear layers, and from the sidewalls. Moreover, these vortices were shed simultaneously from each side, suggesting that the entire vortex ring was convected as a whole and eventually broke down to turbulence.

Influence of the Reynolds number

The Reynolds number had little influence on the wake topology. As the Reynolds number increased within the range of these experiments, it was followed by an increase in the turbulence intensity, but the structural organization of the wake remained the same. As an example, Fig. 9 shows the lower vortex (C2) had essentially the same form in the Re_L range from 7000 to 27700. This is not surprising as the location of flow separation is insensitive to the Reynolds number and is fixed by the geometry of the vehicle (Wassen and Thiele, 2008).

Figure 9: Flow visualization of the bottom vortex branch at Re_L = 7000 (a), 9700 (b), 13800 (c), 20800 (d), and 27700 (e).

CONCLUSIONS

This study has documented qualitatively and, in part, quantitatively, the vortical structure of the near-wake of a square-back vehicle model mounted on both a fixed and a moving ground. Flow separation and vortex generation mechanisms have been observed and analyzed comparatively.

The near-wake was found to contain a main vortex-ring-like structure, as demonstrated by the fact that in both the vertical and horizontal mid-planes the recirculation zones were split in two counter-rotating vortices. In the fixed-ground case, in agreement with the literature, the upper part of the vortex ring was found to be stronger than the lower part, which, however, occupied a larger area of the wake. The upper and side parts became detached periodically and were convected downstream, whereas the lower part remained attached. This asymmetric vortex ring detachment implies the generation of quasi-periodic horseshoe-shaped structures propagating away from the model's rear.

The results obtained with a moving floor could not be easily compared to the literature, as there are fewer studies on the subject. The moving floor strongly influences the lower section of the wake and causes the lower vortex to be much more strong than with a fixed ground. In this configuration, the vortex ring that is formed at the base of the vehicle appears to detach quasi-periodically as a whole.

ACKNOWLEDGMENTS

Financial support by the Natural Sciences and Engineering Research Council of Canada (NSERC) is gratefully acknowledged.

REFERENCES

Ahmed, S. (1981). Wake structures of typical automobile shapes. J. Fluids Eng. 103, pp. 162–169.

Aider, J.-L, Beaudoin, J.-F., Wesfreid, J. E. (2010) Drag and lift reduction of a 3D bluff-body using active vortex generators. Exp. Fluids 48, pp. 771–789.

Bailey S. C. C., Martinuzzi R. J., and Kopp G. A. (2002). The effects of wall proximity on vortex shedding from a square cylinder: three-dimensional effects. Phys. Fluids 14, pp. 4160-4177.

Bearman, P. W., D. D. Beer, E. Hamidy, and J. K. Harvey (1989). The effect of a moving floor on wind-tunnel simulation of road vehicles. SAE Paper No. 880245.

Bearman, P. W. (1997). Near wake flows behind two- and three-dimensional bluff bodies. J. Wind Eng. Industr. Aerodyn. 69-71, pp. 33–54.

Bosch G., Kappler M., and Rodi W. (1996). Experiments on the flow past a square cylinder placed near a wall. Exper. Thermal Fluid Sci. 13 (3), pp. 292-305.

Carr, G.W. (1983). Potential for aerodynamic drag reduction in car design. Int. J. of Vehicle Design, Technological Advances in Vehicle Design Series, SP3, *Impact of Aerodynamics on Vehicle Design*, pp. 173-196.

Cogotti, A. (1983). Aerodynamic characteristics of car wheels. Int. J. of Vehicle Design, Technological Advances in Vehicle Design Series, SP3, *Impact of Aerodynamics on Vehicle Design,* pp. 173-196.

Gilliéron, P., Kourta, A. (2010). Aerodynamic drag reduction by vertical splitter plates. Exp. Fluids, 48, pp. 1-16.

Gohlke, M., Beaudoin, J.F., Amielh, M., Anselmet, F. (2007). Experimental analysis of flow structures and forces on a 3D-bluff-body in constant cross-wind. Exp. Fluids 43, pp. 579-594.

Guilmineau, E., (2008). Computational study of flow around a simplified car body. J. Wind Eng. Industr. Aerodyn. 96, pp. 1207–1217.

Guilmineau, E., Chometon, F., (2009). Effect of side wind on a simplified car model: Experimental and numerical analysis. J. Fluids Eng. 131 (021104).

Howell, J. (2005). SUV aerodynamics. VKI Lecture Series 2005-05, *Road Vehicle Aerodynamics*.

Hucho W.H., and Sovran G. (1993). Aerodynamics of road vehicles. Annu. Rev. Fluid Mech. 25, pp. 485-537.

Krajnovic, S., and Davidson, L., (2005). Flow around a simplified car, Part 2: Understanding the flow. J. Fluids Eng. 127, pp. 919-928.

Martinuzzi, R., and Tropea, C. (1993). The flow around surface-mounted prismatic obstacles placed in fully developed channel flow. J. Fluids Eng. 115, pp. 85-91.

Rouméas M., Gilliéron P., and Kourta A. (2009). Analysis and control of the near-wake flow over a square-back geometry. Comp. Fluids 38, pp. 60-70.

Shah, K.B., and Ferziger, J.H. (1997). A fluid mechanicians view of wind engineering: Large eddy simulation of flow past a cubic obstacle. J. Wind Eng. Industr. Aerodyn. 67, pp. 211-224.

Wassen, E., Thiele, F. (2008). Drag reduction for a generic car model using steady blowing. AIAA 2008-3771. 4th Flow Control Conference, Seattle, Washington.